Clinical Kidney Journal

Clinical Kidney Journal, 2024, vol. 17, no. 8, sfae221

https://doi.org/10.1093/ckj/sfae221
Advance Access Publication Date: 16 July 2024
Original Article

ORIGINAL ARTICLE

Urine metabolite changes after cardiac surgery predict acute kidney injury

Qi Zeng[1,*], Jinghan Feng[1,*], Xinni Zhang[1], Fangyuan Peng[1], Ting Ren[1], Zhouping Zou[1], Chao Tang[1], Qian Sun[1], Xiaoqiang Ding[1,2,3,4,5] and Ping Jia[1,2]

[1]Division of Nephrology, Zhongshan Hospital, Fudan University, Shanghai, China, [2]Shanghai Medical Center of Kidney, Shanghai, China, [3]Kidney and Dialysis Institute of Shanghai, Shanghai, China, [4]Kidney and Blood Purification Laboratory of Shanghai, Shanghai, China and [5]Hemodialysis Quality Control Center of Shanghai, Shanghai, China

*These authors contributed equally to this work.
Correspondence to: Ping Jia; E-mail: jia.ping1@zs-hospital.sh.cn, Xiaoqiang Ding; E-mail: ding.xiaoqiang@zs-hospital.sh.cn

ABSTRACT

Background. Acute kidney injury (AKI) is a serious complication in patients undergoing cardiac surgery, with the underlying mechanism remaining elusive and a lack of specific biomarkers for cardiac surgery-associated AKI (CS-AKI).
Methods. We performed an untargeted metabolomics analysis of urine samples procured from a cohort of patients with or without AKI at 6 and 24 h following cardiac surgery. Based on the differential urinary metabolites discovered, we further examined the expressions of the key metabolic enzymes that regulate these metabolites in kidney during AKI using a mouse model of ischemia–reperfusion injury (IRI) and in hypoxia-treated tubular epithelial cells (TECs).
Results. The urine metabolomic profiles in AKI patients were significantly different from those in non-AKI patients, including upregulation of tryptophan metabolism– and aerobic glycolysis–related metabolites, such as L-tryptophan and D-glucose-1-phosphate, and downregulation of fatty acid oxidation (FAO) and tricarboxylic acid (TCA) cycle–related metabolites. Spearman correlation analysis showed that serum creatinine was positively correlated with urinary L-tryptophan and indole, which had high accuracy for predicting AKI. In animal experiments, we demonstrated that the expression of rate-limiting enzymes in glycolysis, such as hexokinase II (HK2), was significantly upregulated during renal IRI. However, the TCA cycle–related key enzyme citrate synthase was significantly downregulated after IRI. *In vitro*, hypoxia induced downregulation of citrate synthase in TECs. In addition, FAO-related gene peroxisome proliferator-activated receptor alpha (PPARα) was remarkably downregulated in kidney during renal IRI.
Conclusion. This study presents urinary metabolites related to CS-AKI, indicating the rewiring of the metabolism in kidney during AKI, identifying potential AKI biomarkers.

Received: 25.1.2024; Editorial decision: 1.7.2024

GRAPHICAL ABSTRACT

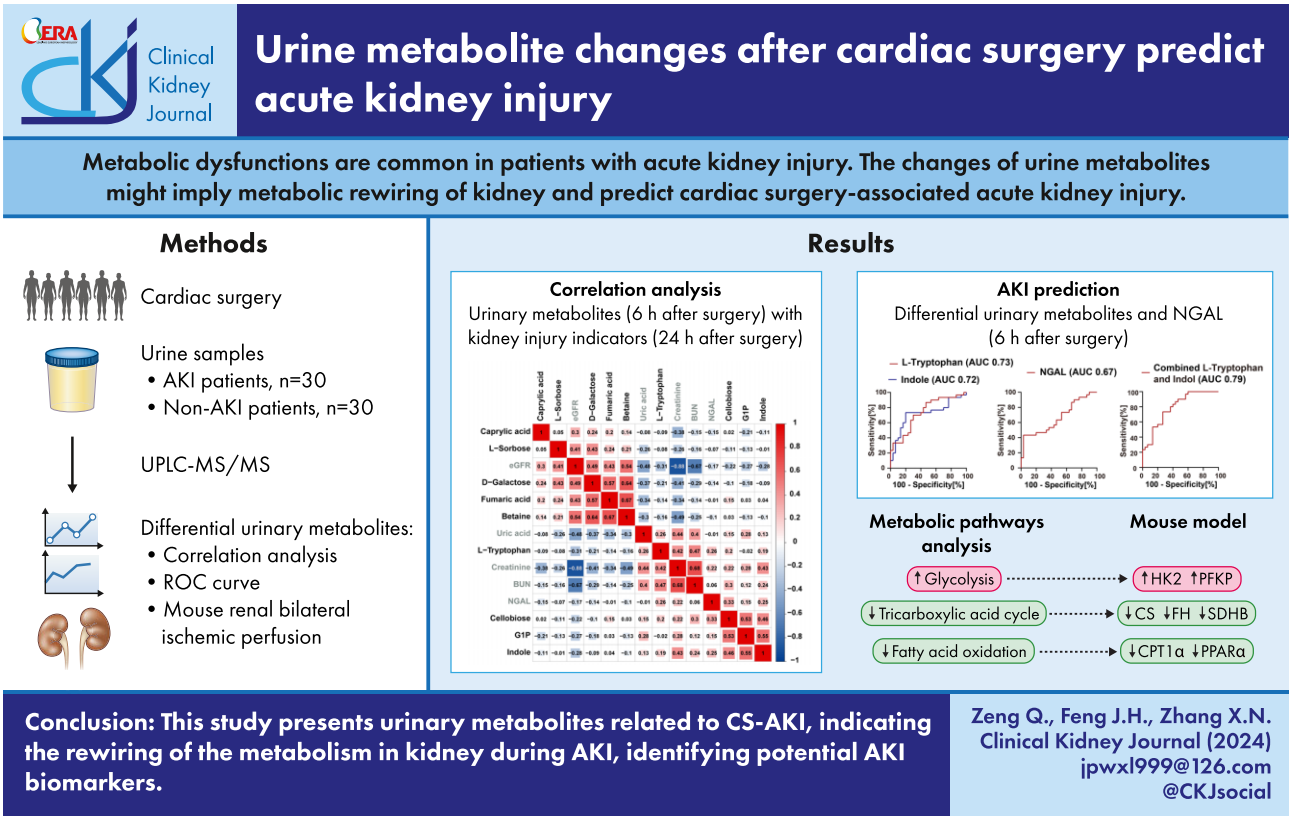

Keywords: acute kidney injury, cardiac surgery, metabolomics, urine metabolites

KEY LEARNING POINTS

What was known:

- Prediction of cardiac surgery-associated acute kidney injury (CS-AKI) remains a challenge.

This study adds:

- Our study aimed to identify urinary metabolites for prediction of CS-AKI, and explore renal metabolism during AKI.

Potential impact:

- We identified differential urinary metabolites associated with metabolic rewiring of kidney.
- Experimental studies demonstrated that abnormal metabolic adaptations contribute to AKI.
- Urinary metabolites could be early indicators of CS-AKI.

INTRODUCTION

Acute kidney injury (AKI) is a clinical syndrome characterized by a sudden decline in renal function, and is commonly observed in adult patients undergoing cardiac surgery. Cardiac surgery-associated AKI (CS-AKI) is the second most common type of AKI after septic AKI in intensive care units, with an incidence of 25%–40% [1], and is associated with high morbidity and mortality rates, prolonged mechanical ventilation, increased hospitalization stay and costs, and development of chronic kidney disease [2–4]. Early identification of patients at high risk of CS-AKI enables clinicians to initiate efficient prevention and treatment measures to reduce the incidence of AKI. So far, the clinical diagnosis of AKI primarily relies on serum creatinine (Scr) levels and urine output [5]. However, variations in Scr level typically occur after renal dysfunction and can also be influenced by several factors including steroids, nutrition and muscle injury, and therefore it does not promptly and accurately reflect the extent of kidney injury. Furthermore, factors like the use of diuretics and bladder capacity can influence urine output [6].

Recent studies have identified several biomarkers for kidney damage, such as neutrophil gelatinase-associated lipocalin (NGAL), kidney injury molecule-1, cystatin C, interleukin-18,

liver fatty acid binding protein, and so on [7, 8]. In particular, NGAL has been used frequently in diagnosis and severity assessment in kidney diseases [9]. Nevertheless, these biomarkers exhibit limitations regarding data stability, clinical reliability and the breadth of the applicable population [10]. Thus, novel specific biomarkers for early diagnosis of CS-AKI are needed.

Clarifying the pathogenesis of CS-AKI is essential to explore specific early diagnostic biomarkers. The pathophysiology of CS-AKI is complex and remains incompletely understood. Renal hypoperfusion and ischemia–reperfusion injury (IRI) are the major injury pathways involved in the development of CS-AKI [11], which induces mitochondrial damage and dysfunction, and metabolism impairment in tubular epithelial cells (TECs), which subsequently leads to cell injury or cell death. Under physiological conditions, TECs primarily rely on oxidative phosphorylation driven by fatty acid oxidation (FAO) to generate energy. In response to ischemic stress, TEC mitochondrial function and metabolism is disturbed, and the ability of TECs to use FAO is impaired, switching to anaerobic glycolysis for energy demand. Abnormal metabolic adaptations of TECs will result in impairment of cell function and survival, contributing to AKI. Alterations in metabolite level typically manifest in biological fluids before the appearance of clinical symptoms during AKI, making their detection valuable for analyzing mechanisms, onset and prognosis of AKI [12]. Given that low molecular weight compounds are usually freely filtered into urine, urine samples serve as ideal candidates for metabolomics research. This is due to several advantages in clinical practice, including non-invasiveness, large sample sizes, easy access and the feasibility of time series analysis [13]. Currently, urine metabolomics is widely adopted as a method for studying kidney diseases.

In this study, we perform an untargeted metabolomics analysis of urine samples procured from a cohort of post-cardiac surgery patients with or without AKI, using liquid chromatography-mass spectrometry (LC-MS). Based on the differential urinary metabolites detected, we further determine the expressions of the key metabolic enzymes that regulates these metabolites in kidney during AKI using a mouse model of IRI and in hypoxia-treated tubular epithelial cells *in vitro*, to explore the rewiring of the metabolism in the pathophysiology of AKI, and identify its potential diagnostic markers.

MATERIALS AND METHODS

Patients

Participants involved in this study (nested case–control study) originated from a prospective cohort study (ChiCTR2000035568) that was conducted to evaluate the early diagnostic biomarkers of AKI on patients undergoing cardiac surgery between 29 June 2021 and 24 February 2022 in Zhongshan Hospital Fudan University. After the completion of the original cohort study, we included the first 30 patients identified as AKI cases and 30 patients without AKI, matched by age and sex, were randomly selected from the same period using SPSS. AKI in this study was defined as an increase in serum creatinine of $\geq$0.3 mg/dL (or 26.5 μmol/L) from baseline within 48 h after cardiac surgery. Eligible patients were adults at high risk for AKI who underwent elective cardiopulmonary bypass cardiac surgery. Exclusion criteria were end-stage kidney disease [estimated glomerular filtration rate (eGFR) of $<$15 mL/min/1.73 m^2 of body-surface area], preexisting AKI, kidney transplantation and pregnancy. All patients signed informed consent.

UPLC-MS/MS measurement of urinary metabolites

Urine samples were collected before cardiac surgery, at 6 and 24 h after surgery, respectively, from AKI and non-AKI patients, used for LC-MS analysis [14]. To assess the repeatability and stability of the entire LC-MS process, 10 μL of each sample was incorporated into the quality control (QC) samples. The LC analysis was conducted using a Vanquish UHPLC System (Thermo Fisher Scientific, USA). The chromatographic separation was conducted using an ACQUITY UPLC® HSS T3 column (150 $\times$ 2.1 mm, 1.8 μm) from Waters (Milford, MA, USA). The column was maintained at 40°C with a flow rate of 0.25 mL/min and an injection volume of 2 μL. For LC-ESI(+)-MS analysis, the mobile phase was composed of 0.1% formic acid in acetonitrile (v/v) and 0.1% formic acid in water (v/v). For LC-ESI(–)-MS analysis, the analyses were processed with acetonitrile and 5 mM ammonium format [15].

The detection of metabolites via mass spectrometry was conducted using an OrbitrapExploris 120 (Thermo Fisher Scientific, USA) equipped with an ESI ion source. We employed simultaneous acquisition of MS1 and MS/MS data (in Full MS-ddMS2 mode, data-dependent MS/MS). The parameters were set as follow: sheath gas pressure (30 arb), auxiliary gas flow (10 arb), spray voltage [3.50 kV for ESI(+) and $-$2.50 kV for ESI(−)], capillary temperature (325°C), MS1 range (m/z 100–1000), MS1 resolving power (60 000 FWHM), number of data-dependent scans per cycle (4), MS/MS resolving power (15 000 FWHM), normalized collision energy (30%) and dynamic exclusion time (automatic) [16].

Data processing and analysis

The raw data involved were converted to mzXML format using MSConvert from ProteoWizard software package (v3.0.8789) [17], followed by processing with XCMS [18] for feature detection, retention time correction and alignment. Metabolite identification was accomplished using accurate mass ($<$30 ppm) and MS/MS data, with matches sought in databases such as Human Metabolome Database (HMDB), MassBank [19], LipidMaps [20], mzCloud [21] and Kyoto Encyclopedia of Genes and Genomes (KEGG) [22]. To correct for any systematic bias, quality control-the robust LOESS signal correction (QC-RLSC) method was applied for data normalization [23]. Post-normalization, only ion peaks displaying relative standard deviations (RSDs) in QC of $<$30% were retained, ensuring accurate metabolite identification.

All multivariate data analyses and modeling were conducted using the Ropls software. Following data scaling, models were constructed using principal component analysis (PCA), partial least-square discriminant analysis (PLS-DA) and orthogonal partial least-square discriminant analysis (OPLS-DA). The metabolic profiles were visualized in a score plot, with each point representing a distinct sample. All evaluated models underwent permutation tests to check for overfitting. Discriminating metabolites were identified using the variable importance (VIP) on projection parameter in the OPLS-DA model. Pathway analysis of the differential metabolites was performed using MetaboAnalyst. The metabolites identified through metabolomics were subsequently mapped onto the KEGG pathway to facilitate interpretation of biological functions.

Animals and animal experiment

All experimental protocols were approved by the Institutional Animal Care and Use Committee of Fudan University. Male mice (C57BL/6, 8–10 weeks old), were obtained commercially from the

Animal Resource Center of Fudan University. Regular mice used in this study were housed under 14-h light/10-h dark cycle and controlled temperature (22–24°C) with free access to food and water.

Mice were randomly assigned to sham-operated or IRI group. Based on our previous studies, renal IRI was induced by bilateral renal pedicle clamping for 30 min [24]. Sham-operated mice underwent the same surgical procedures but without occlusion of renal pedicle. Mice were euthanized at 6, 12 and 24 h separately after the operation, and kidney samples were collected.

Cell culture

Mouse renal TECs were purchased from BeNa Culture Collection (BNCC, China), and cultured in RPMI 1640 medium supplemented with 10% fetal bovine serum, grown in cell incubators at 37°C and 5% CO_2 atmosphere.

Hypoxia and reoxygenation treatment

To induced hypoxia, the cells were changed to serum-free RPMI1640 medium and incubated in a cell hypoxia incubator with 1% O_2, 5% CO_2 and 94% N_2 at 37°C. After 24 h of hypoxia, TECs were transferred back to normoxic incubators for reoxygenation for 4 h.

Real-time polymerase chain reaction

Total RNA was extracted from TECs and mouse kidney using Trizol reagent (T9424l; Sigma-Aldrich). After reverse transcription to cDNA (PrimeScript RT reagent Kit; TaKaRa), polymerase chain reaction (PCR) was performed using SYBR® Premix Ex TaqTM II (DRR081A; TaKaRa). The target gene expression was quantified to that of the internal control gene (β-actin) based on the comparison of the threshold cycle (CT) at constant fluorescence intensity. Relative expression was calculated using the $2^{-\Delta\Delta Ct}$ method. The specific primers sequences are provided in Supplementary data, Table S1.

Western blotting

Western blot was performed as previously described [25]. The primary1 antibodies used in this study were rabbit anti-Hexokinase II (C64G5; Cell Signaling Technology, 1:1000), rabbit anti-citrate synthetase antibody (ab96600; Abcam), mouse anti-fumarate hydratase (H-6, Santa Cruz Biotechnology), mouse anti-SDHB (ab14714; Abcam) and mouse anti-beta Actin (KC-5A08; Aksomics). Anti-rabbit immunoglobulin G (IgG) or anti-mouse IgG was used as a secondary antibody.

Immunofluorescence

Immunofluorescence staining was performed on frozen sections of the mouse kidney, as previously described [26], or using TSA 3-color kit (RC0086-23RM, Recordbio) according to the manufacturer's instruction. The sections were incubated with primary antibodies: Lotus tetragonolobus lectin (LTL; FL-1321, Vector Laboratories, Burlingame, CA, USA), rabbit anti-Aquaporin 1 antibody (ab168387; Abcam), rabbit anti-Aquaporin 2 antibody (ab199975; Abcam), rabbit anti-UMOD antibody (ab207170; Abcam) and anti-NCC (AB3553; Merck-millipore), at 4°C overnight. After three washing steps, the sections were incubated with appropriate secondary antibodies (Donkey anti-Rabbit IgG-AlexaFluor 488/594, Absin; Alexa Fluor® 488 Streptavidin, Yeasen). Nuclei were stained with DAPI (0100-20; Southern Biotech). Images were obtained using a confocal microscope (ZeissLSM 700).

Table 1: Basic characteristics and preoperative examinations.

Characteristics	No AKI ($n = 30$)	AKI ($n = 30$)	P-value
Age, years	65.3 ± 6.9	64.7 ± 6.7	.735
Men, No. (%)	21 (70.0)	20 (66.7)	.781
Smoking, No. (%)	6 (20.0)	11 (36.7)	.152
Alcohol consumption, No. (%)	9 (30.0)	9 (30.0)	1.000
Medication, No. (%)			
ACEI or ARBs	9 (30.0)	7 (23.3)	.559
Diuretics	13 (43.3)	12 (40.0)	.793
Insulin therapy	0 (0.0)	2 (6.7)	.492
Oral antidiabetic drugs	1 (3.3)	1 (3.3)	1.000
Cholesterol-lowering drug	3 (10.0)	6 (20.0)	.472
Comorbidities, No. (%)			
Hypertension	8 (26.7)	14 (46.7)	.108
Diabetes mellitus	1 (3.3)	5 (16.7)	.195
Chronic kidney disease	1 (3.3)	0 (0.0)	1.000
Hyperuricemia	3 (10.0)	4 (13.3)	1.000
NYHA classification, No. (%)			
I–II	9 (30.0)	10 (33.3)	.781
III–IV	21 (70.0)	20 (66.7)	
Clinical examinations			
Hb (g/L)	132 ± 21	129 ± 17	.274
Albumin (g/L)	40.4 ± 3.3	40.8 ± 2.9	.532
BUN (mmol/L)	8.43 ± 2.76	8.34 ± 2.30	.947
Scr (μmol//L)	96.3 ± 18.0	96.3 ± 20.2	1.000
eGFR (mL/min/1.73 m^2)	66.6 ± 14.9	68.3 ± 17.5	.756
UA (μmol//L)	433 ± 126	422 ± 112	1.000
TC (mmol/L)	4.14 ± 1.04	4.11 ± 1.02	.859
TG (mmol/L)	1.47 ± 1.36	1.33 ± 0.78	.836
LDL-c (mmol/L)	2.41 ± 0.86	2.23 ± 0.85	.322

Data are presented as mean (± standard deviation) or n (%).
Chronic kidney disease: estimated glomerular filtration rate (eGFR) <60 mL/kg.m^2.
NYHA, New York Heart Association; RIPC, remote ischemic post-conditioning; ACEI, angiotensin-converting enzyme inhibitor; ARB, angiotensin-receptor blocker; Hb, hemoglobin; UA, uric acid; TC, total cholesterol; TG, triglycerides; LDL, low-density lipoprotein.

Enzyme-linked immunosorbent assay

Concentration of urine NGAL was measured using commercially available enzyme-linked immunosorbent assay kits (QK1757, R&D Systems), according to the manufacturer's protocol.

Statistical analysis

All statistical analyses were performed using SPSS (20.0), MedCalc (8.0) and GraphpadPrism (9.0). Data are presented as mean ± standard deviation or counts (percentages). Comparisons between two groups were tested using unpaired t-test or Pearson's chi-squared test. For multiple comparisons, one-way analysis of variance followed by a Bonferroni posttest were used.

Spearman's correlation was calculated between specific metabolites, the kidney injury indicators and other clinical parameters. Receiver operating characteristics curve (ROC) analysis was performed, and the area under the curve (AUC) was calculated to find the best urine metabolites that can predict AKI effectively. A P-value <.05 was defined as statistically significant.

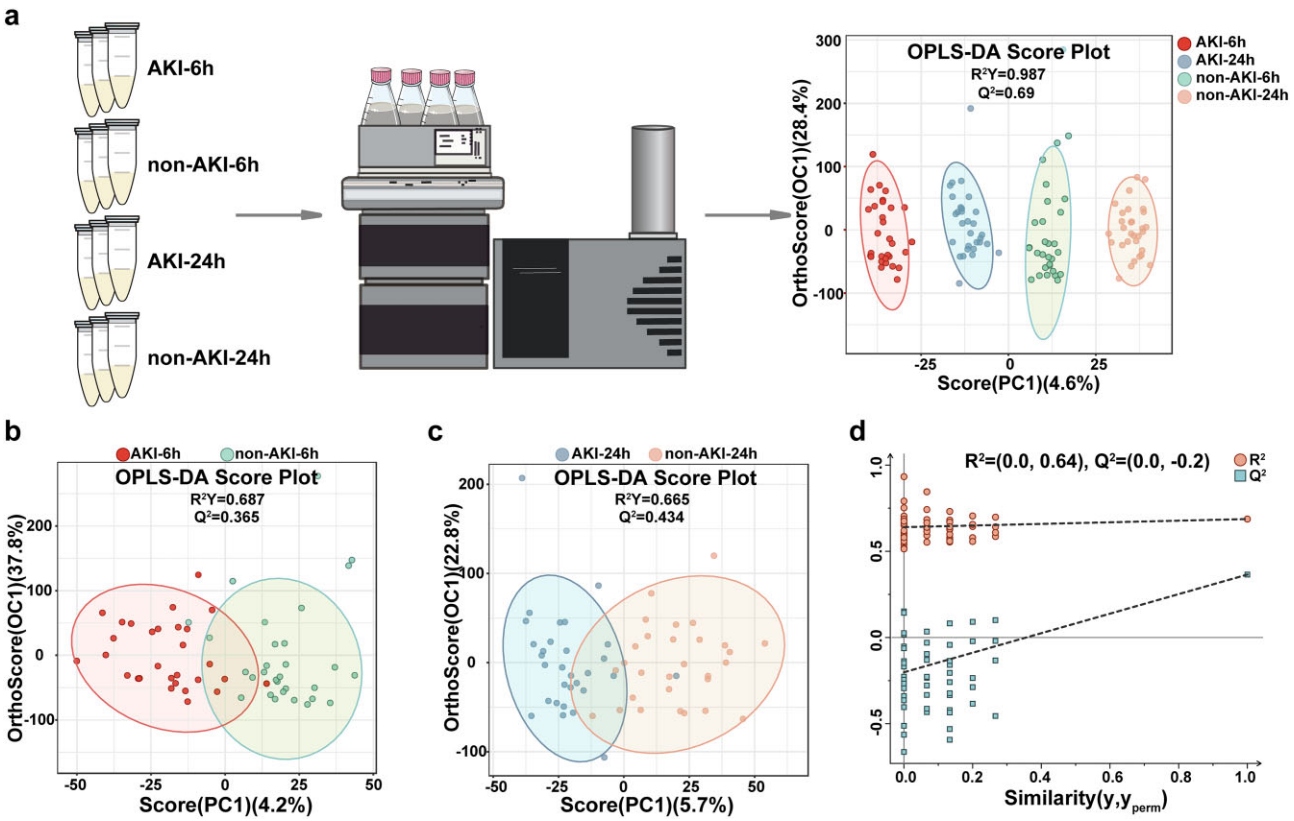

Figure 1: Plots of OPLS-DA score and permutation test for urine metabolomics in AKI and non-AKI patients. (**a**) Grouping and schematic diagram of urine metabolomics. OPLS-DA score plot in AKI-6h group (red), non-AKI-6h group (green), AKI-24h group (blue) and non-AKI-24h group (orange). (**b**) Comparison of urine metabolic profiles at 6 h in AKI patients and non-AKI patients. (**c**) Comparison of urine metabolic profiles at 24 h in AKI patients and non-AKI patients. (**d**) OPLS-DA permutation test plot in positive ion mode of AKI-6h and non-AKI-6h. The criterion for assessing non-overfitting in an OPLS-DA model is that the regression line of the Q^2 values, represented by blue points, passes through the origin or has a negative intercept on the y-axis.

RESULTS

Patients' clinical data

The basic characteristics and preoperative clinical indicators of the AKI and non-AKI patients are shown in Table 1. The two groups were well matched in baseline demographic and clinical indicators. There were no significant differences in comorbidities, baseline medications including drugs with a potential effect on renal function, and preoperative indicators including hemoglobin, serum alanine aminotransferase and renal function indexes such as creatinine, blood urea nitrogen (BUN) and eGFR.

Multivariate statistical analysis of metabolites

All samples were analyzed in both positive and negative ion modes using UPLC-MS/MS, followed by multivariate statistical analysis of the processed data. For the QC samples, approximately 65% exhibited characteristic peak RSD values of <30%, underscoring the high quality of these samples [16] (Supplementary data, Fig. S1a). The PCA score plot displayed the original state of all sample data, where the urine components from the four groups could not be distinctly separated, as illustrated in Supplementary data, Fig. S1b. The OPLS-DA method was able to completely differentiate the four groups based on their metabolic profiles, exhibiting moderate reproducibility during cross-validation ($R^2 = 0.987$; $Q^2 = 0.69$) (Fig. 1a). The metabolic profiles at 6 h (Fig. 1b) and 24 h (Fig. 1c) exhibited significant differences between the AKI and non-AKI groups, with little overlap. Moreover, the validity of the constructed OPLS-DA model, free from overfitting, was confirmed through a permutation test (Fig. 1d).

Differential urinary metabolites and metabolic pathways between AKI croup and non-AKI group

We performed OPLS-DA to screen the significantly differential metabolites, employing VIP >1 and *P*-value <.05 as screening criteria to identify differential metabolites. We detected a total of 818 metabolites, observed 93 differential metabolites between AKI-6h group and non-AKI-6h group, namely 44 upregulated and 49 downregulated metabolites in the AKI-6h group. We also identified 115 differential metabolites between the AKI-24h group and non-AKI-24h group, 40 of which were also involved in the AKI-6h and non-AKI-6h groups. Among these differential metabolites, we found that D-glucose-1-phosphate (a product of glycogen breakdown involved in various carbohydrate metabolisms), beta-D-fructose-6-phosphate (intermediate product of glycolysis), L-tryptophan (an essential amino acid involved in generating serotonin, indole, etc., and associated with immune regulation) and cellobiose (intermediate product of starch and sucrose metabolism) were significantly upregulated in the AKI group. However, betaine (an alkaloid that assists in maintaining kidney osmotic pressure), fumaric acid (an

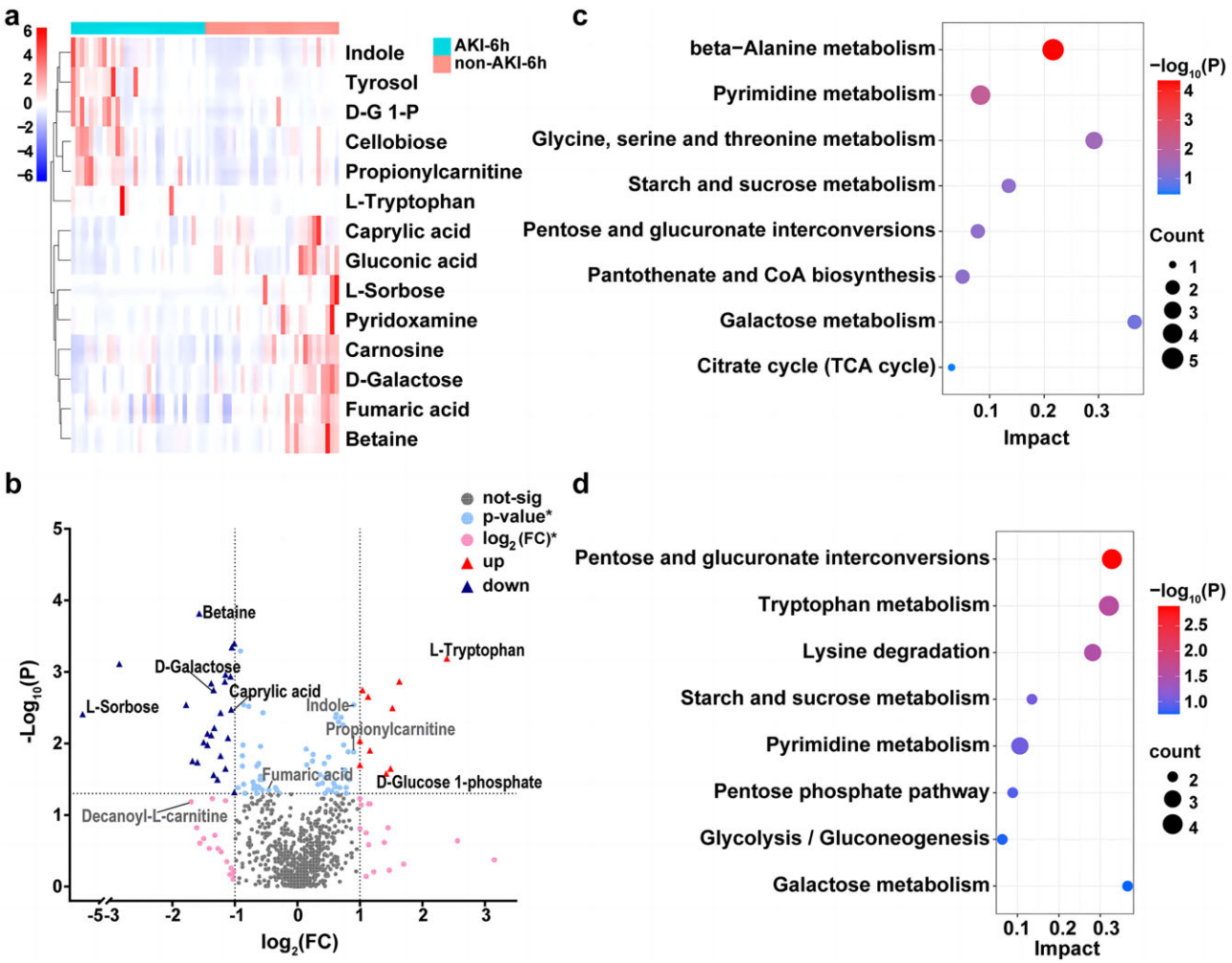

Figure 2: Multivariate statistical analysis of metabolites. (**a**) Heat map of differential metabolites between the AKI-6h group and non-AKI-6h group. The columns represent samples, rows represent metabolites. The relative content of the metabolites is displayed by color. (**b**) Volcano map of differential metabolites between AKI-6h and non-AKI-6h, with |Log2(FC)|=1 and *P*-value = .05 as the boundary. Red triangles represent upregulated metabolites with significant differences, while dark blue ones represent significantly downregulated metabolites. Metabolites only with significant FC are presented as pink dots, those only with significant *P*-value are presented as light blue dots and those without significance are grey dots. (c, d) Bubble diagram of enriched pathways of metabolites between AKI and non-AKI at 6 h (**c**) or 24 h (**d**). Pathway impact, or centrality, is measured based on topological assessment. As the color gradient ranked by −log10 (*P*-value) shows, the color of bubbles represents the significance of a pathway, and the size represents the hits number.

intermediate product of the TCA cycle), caprylic acid (a 9-C saturated fatty acid) and L-carnitine (a mediator of fatty acid transport into mitochondria) were downregulated in AKI (Fig. 2a and b).

We utilized the MetaboAnalyst database for pathway enrichment analysis of the differential metabolites in urine, identified 29 and 35 upregulated metabolic pathways at 6 and 24 h in the AKI group, respectively, compared with the non-AKI group, including Starch and Sucrose metabolism, Pentose and Glucoronate interconversions, Galactose metabolism, and Pyrimidine metabolism, which were both activated at 6 and 24 h in AKI group (Fig. 2c and d; Supplementary data, Tables S2 and S3). Glycolysis/Gluconeogenesis and Tryptophan metabolism pathways were significantly activated at 24 h in the AKI group (Supplementary data, Table S3). In particular, in Tryptophan metabolism, a panel of four differential metabolites encompassing L-tryptophan, indole, xanthurenic acid and L-formyl kynurenine were markedly upregulated in the AKI groups (Fig. 3). Metabolites enriched in these pathways are delineated in Supplementary data, Tables S2 and S3.

Correlation of differential metabolites and the kidney injury indicators

To elucidate the correlation between the differential metabolites and clinical biochemical indicators (Scr, eGFR, BUN), we conducted a Spearman correlation analysis. As depicted in Fig. 4, there was a significant positive correlation between creatinine and urinary L-tryptophan, indole, and a negative correlation between serum and urinary betaine, D-galactose. Accordingly, eGFR was negatively correlated with urinary L-sorbose, D-galactose, betaine and fumaric acid. BUN exhibited a positive correlation with L-tryptophan. Additionally, positive correlations were observed between D-galactose and betaine ($r = 0.64$), as well as between fumaric acid and betaine ($r = 0.67$).

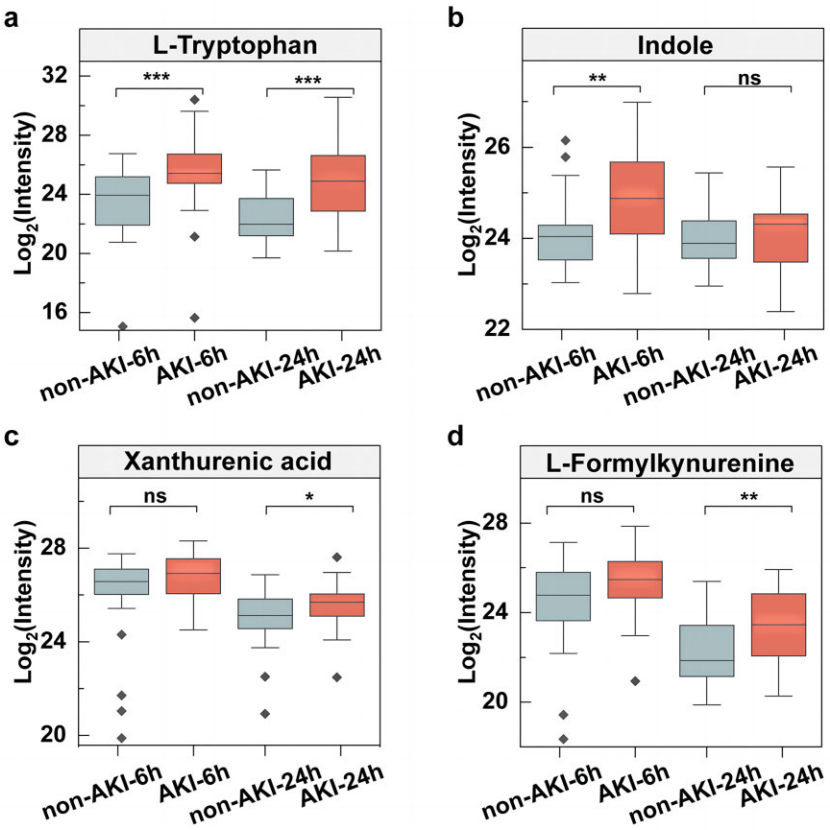

Figure 3: Concentrations of urinary metabolites in tryptophan metabolism in AKI and non-AKI patients. Concentrations of urinary L-tryptophan (**a**), indole (**b**), xanthurenic acid (**c**) and L-formyl kynurenine (**d**) at 6 and 24 h in AKI and non-AKI patients. $^{*}P < .05$, $^{**}P < .01$, $^{***}P < .001$.

L-Tryptophan is an essential amino acid and serves as a precursor for many significant biomolecules. In the kidneys, L-tryptophan and its metabolites perform complex functions, playing crucial roles in regulating renal blood flow and immune responses [27]. D-Glucose-1-phosphate is a glucose molecule with a phosphate group attached to the first carbon atom. It serves as an intermediate in glycogenolysis, where it is released by glycogen phosphorylase and participates in glycolysis, gluconeogenesis and the pentose phosphate pathway [28]. β-D-Fructose 6-phosphate is a fructose molecule with a phosphate group attached to the sixth carbon atom. In the kidneys, β-D-fructose-6-phosphate supports energy metabolism and regulation, ensuring adequate energy supply for the high demands of tubular reabsorption and filtration processes [29].

Urine metabolites for prediction of AKI

Based on the detected differential metabolites, we identified representative urine metabolites associated with amino acid metabolism, glycolysis and fatty acid oxidation for predicting CS-AKI. Four metabolites including L-tryptophan, indole, D-glucose-1-phosphate and beta-D-fructose-6-phosphate were selected. We then performed ROC analysis of these metabolites for predicting CS-AKI, and found that L-tryptophan and indole, involved in amino acid metabolism, presented high accuracy and the AUC were 0.73 [95% confidence interval (CI) 0.61–0.86] and 0.72 (95% CI 0.58–0.85) (Fig. 5a). D-Glucose-1-phosphate and beta-D-fructose-6-phosphate were glucose metabolism–related metabolites, with AUC values of 0.65 (95% CI 0.52–0.79) and 0.60 (95% CI 0.46–0.75) (Fig. 5b). Binary logistic regression was used to build metabolite models for predicting AKI. Metabolite Models 1 to 2 consisted of two metabolites (L-tryptophan and indole, L-tryptophan and D-glucose-1-phosphate). The AUC of all metabolism models were higher than that of NGAL (Fig. 5c and d). In addition, we detected the concentration of NGAL in urine, which was often used as a diagnostic biomarker of AKI, and found that urinary NGAL was significantly increased in AKI patients at 6 h after cardiac surgery (Supplementary data, Fig. S2), with an AUC of 0.67 (95% CI 0.53–0.80) (Fig. 5e). The details of sensitivity, specificity and related CIs for cut-off value are presented in Supplementary data, Table S4. Taken together, our results demonstrated that urinary metabolites, especially L-tryptophan and indole have higher capacity of prediction for CS-AKI than urinary NGAL. These metabolites and metabolite models in our study might be potential biomarkers for CS-AKI.

Aerobic glycolysis is activated in kidney during AKI

In our study, we observed an increase in glucose-1-phosphate, which partakes in glycolysis by interconverting with glucose-6-phosphate, in urine at 6 h after cardiac surgery in the AKI group. This elevation became more pronounced at 24 h after cardiac surgery. Meanwhile, fructose-6-phosphate was also significantly increased in urine at 24 h in AKI patients (Fig. 6a). These findings imply an alteration of glycolysis in kidney in the presence of AKI. To confirm this metabolic alteration, we established a mouse model of renal IRI, and examined the expression of hexokinase II (HK2) and platelet-type phosphofructose kinase (PFKP), two

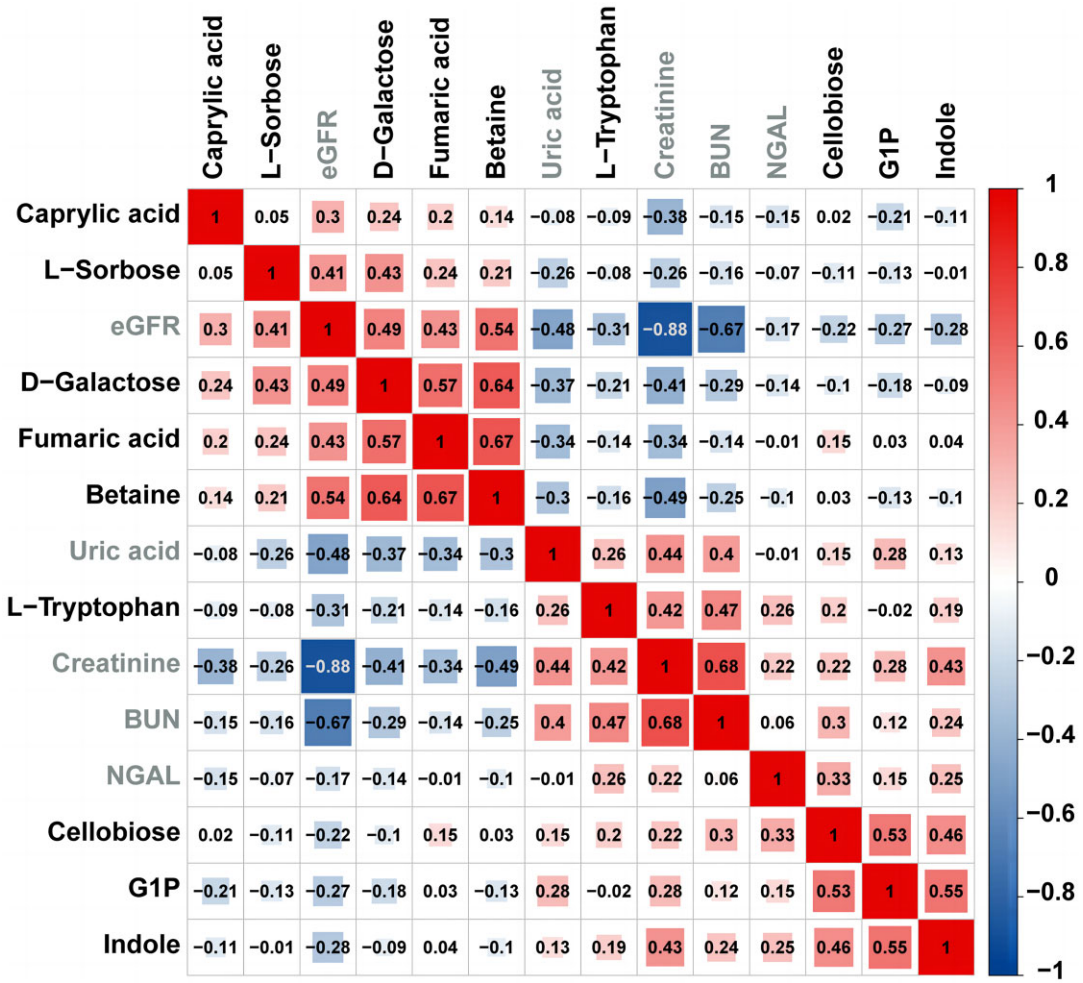

Figure 4: Correlation of differential metabolites and the kidney injury indicators. Red color indicates a positive correlation, blue color indicates a negative correlation; the depth of the color and the size of the color block indicate the strength of the correlation. The number in the block indicates the correlation coefficient. Blood renal function (including BUN, creatinine, eGFR, uric acid) was measured 24 h after surgery. Urine NGAL and metabolites were measured at 6 h early after cardiac surgery.

rate-limiting enzymes in glycolysis which catalyze the conversion of glucose to glucose-6-phosphate, and fructose-6-phosphate to fructose 1,6-bisphosphate, respectively. The results revealed that HK2 was significantly upregulated in kidney at 6 h after IRI, and remained high level until 24 h (Fig. 6b and c). The protein expression of PFKP was also upregulated at 6 h after IRI, implying an enhancement of aerobic glycolysis in kidney during AKI. Furthermore, we performed immunofluorescence staining of HK2 and found that HK2 was predominantly localized in proximal tubules (Fig. 6d), suggesting that IRI induces activating of aerobic glycolysis in proximal tubular epithelial cells, the elevated urinary glucose-1-phosphate and fructose-6-phosphate might originate from damaged proximal tubules.

TCA cycling is suppressed in kidney during AKI

There was a significant decrease in urinary fumaric acid (an important intermediate product of the TCA cycle) level at 6 h after cardiac surgery in the AKI group compared with the non-AKI group. In addition, *cis*-aconitic acid, another intermediate product of the TCA cycle, was reduced in the urine of AKI patients, although this did not meet statistical significance ($P = .055$, Fig. 7a). Then, we examined the expression of citrate synthase, iron sulfur subunit of succinate dehydrogenase (SDHB) and fumarate hydratase (FH), which are key enzymes involved in TCA cycle and regulate the expression of *cis*-aconitic acid and fumaric acid. The results showed that these three TCA cycle enzymes were significantly downregulated at both the mRNA and protein levels after IRI (Fig. 7b–e). We performed immunofluorescence staining of the SDHB and found that SDHB was predominantly localized in the proximal tubules (Fig. 7g). Next, we treated TECs with hypoxia and reoxygenation, and found that, in contrast to normoxia treatment, hypoxia and reoxygenation induced significant downregulation of SDHB and citrate synthase in TECs (Fig. 7f). Collectively, these data suggested that TCA cycle was suppressed in proximal tubular epithelial cells during ischemic AKI.

Fatty acid β-oxidation is impaired in kidney during AKI

In our previous study, we demonstrated that fatty acid oxidation was inhibited in kidney during IRI or cisplatin treatment, leading to lipotoxicity characterized by intracellular lipid accumulation and tubular epithelial cell injury. In the present study, our findings revealed that carnitine (a crucial mediator transporting medium- and long-chain fatty acids to mitochondria) was

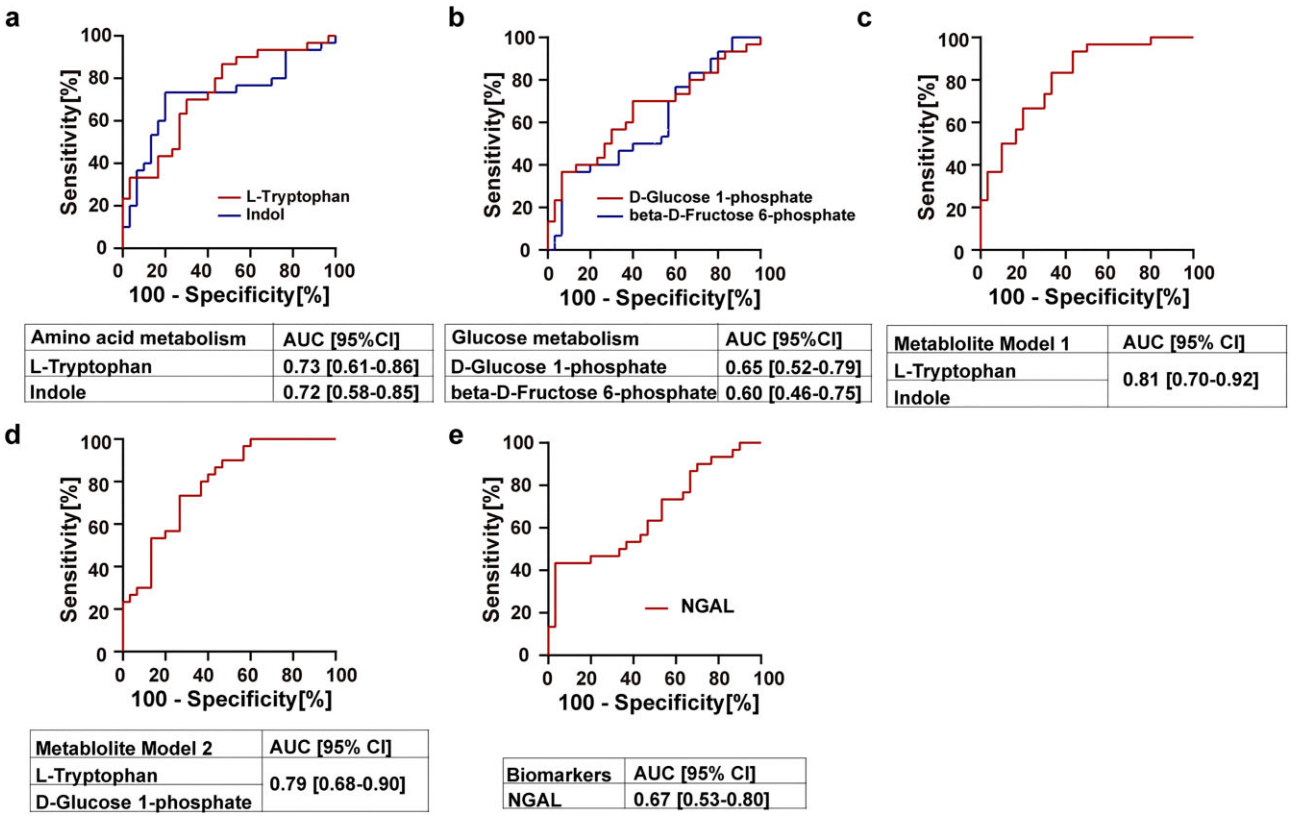

Amino acid metabolism	AUC [95%CI]
L-Tryptophan	0.73 [0.61-0.86]
Indole	0.72 [0.58-0.85]

Glucose metabolism	AUC [95%CI]
D-Glucose 1-phosphate	0.65 [0.52-0.79]
beta-D-Fructose 6-phosphate	0.60 [0.46-0.75]

Metablolite Model 1	AUC [95% CI]
L-Tryptophan	0.81 [0.70-0.92]
Indole	

Metablolite Model 2	AUC [95% CI]
L-Tryptophan	0.79 [0.68-0.90]
D-Glucose 1-phosphate	

Biomarkers	AUC [95% CI]
NGAL	0.67 [0.53-0.80]

Figure 5: ROC curve analysis for prediction of AKI. (**a**) The AUC value of L-tryptophan and indole. (**b**) The AUC value of D-glucose-1-phosphate and beta-D-fructose-6-phosphate. (**c**) Metabolite Model 1: L-tryptophan combined with indole. (**d**) Metabolite Model 2: L-tryptophan combined with D-glucose-1-phosphate. (**e**) The AUC value of NGAL. Urine NGAL and metabolites were measured at 6 h early after cardiac surgery.

markedly decreased in the urine of AKI patients at 6 and 24 h after cardiac surgery (Fig. 8a). Additionally, decanoyl-carnitine, a medium-chain ester acylcarnitine, was reduced in the urine of AKI patients, although this did not meet statistical significance ($P = .065$). Then, we detected expression of the key enzymes regulating fatty acid metabolism, carnitine palmitoyl transferase 1α (CPT1α) and peroxisome proliferator-activated receptor alpha (PPARα), in the kidney of IRI mice. The results showed that CPT1α was downregulated in the time-dependent manner after IRI (Fig. 8b). PPARα was also decreased both in protein and mRNA levels in kidney after renal IRI (Fig. 8c and d). These results imply that reduced carnitine hinders the entry of fatty acids into the mitochondria, subsequently influencing the fatty acids β-oxidation during AKI.

DISCUSSION

In this study, we investigated the urinary metabolic profiles of patients with or without AKI, following cardiac surgery, and identified that D-glucose-1-phosphate, beta-D-fructose-6-phosphate, L-tryptophan and cellobiose were significantly upregulated in the AKI group, while, betaine, fumaric acid, caprylic acid and L-carnitine were downregulated. The alteration of these urinary metabolites was consistent with the metabolic reprogramming of kidney during AKI, including the activation of anaerobic glycolysis, inhibition of TCA cycle and FAO in kidney, providing potential biomarkers for prediction of CS-AKI as well.

The rapid advancements in metabolomics technologies have endowed urine metabolomics with a diverse array of applications encompassing disease diagnosis, identification of novel drug targets, assessment of biomarkers for disease prognosis and evaluation of therapeutic outcomes [30]. Bai *et al.*'s study compared the urine metabolites before and 24 h after surgery in CS-AKI patients through ULPS-LS. They discovered that the differential metabolites were also enriched in amino acid–related metabolic pathways such as tryptophan metabolism, which was consistent with our results. However, Bai did not further analyze the predictive value of differential metabolites [31]. Some studies also focused on finding urine metabolites as novel biomarkers, while lacking comparisons with NGAL and KIM-1. Urine metabolomics conducted by Barrios demonstrated that decreased urine PGI2 and TXA2 concentration in ICU patients might serve as biomarkers for the diagnosis and prognosis of AKI [32]. Some researchers have investigated the predictive value of urine metabolites for AKI on animal models. Their results showed that phenylacetylglycine, a catabolic product of fatty acids, was significantly decreased in urine of septic AKI mice and was correlated with serum NGAL concentration [33].

Previous studies also reveal the advantages of urine metabolites over clinical indicators in CS-AKI prediction. Tian *et al.* conducted urine metabolomics in patients with or without AKI after cardiac surgery, and found that the predictive value of combined five differential metabolites (tyrosyl-gamma-glutamate, arginylarginine, 5-acetylamino-6-amino-3-methyluracil, L-methionine, deoxycholic acid) was significantly

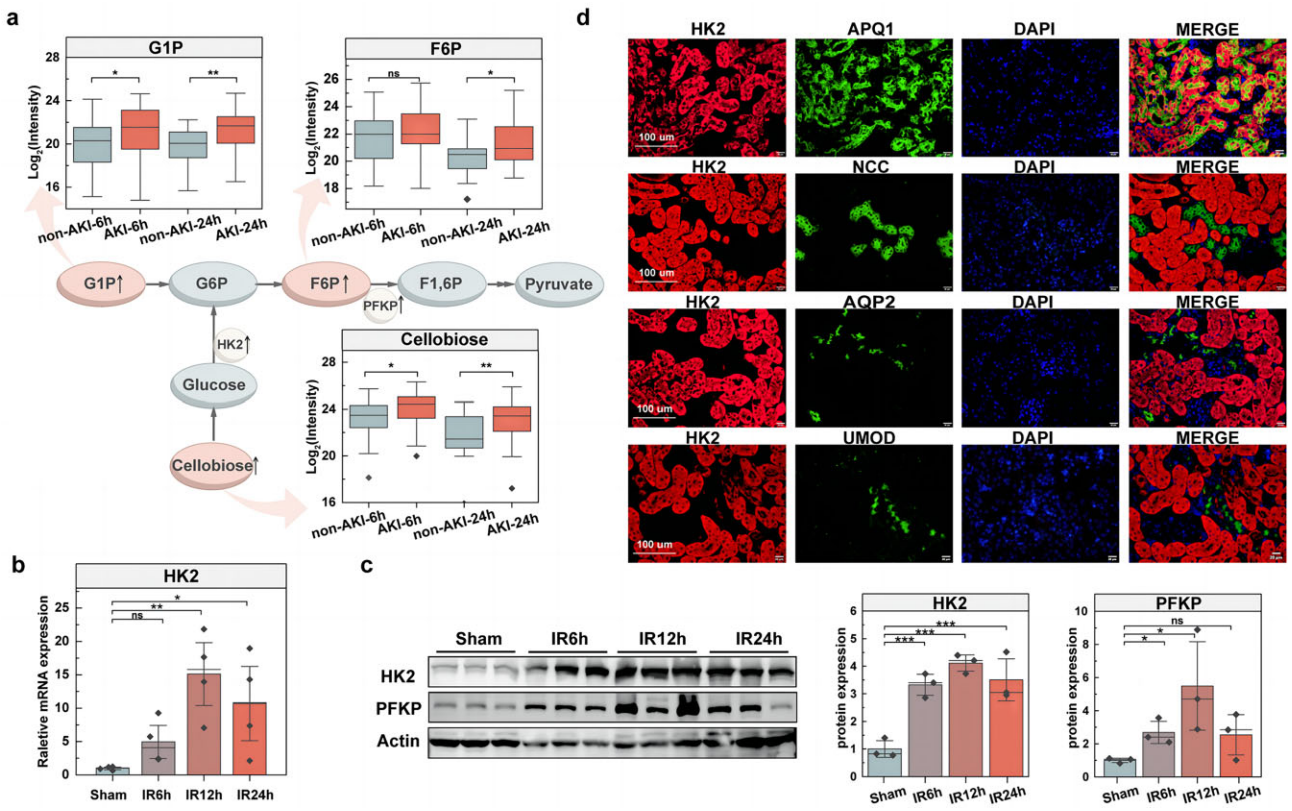

Figure 6: Aerobic glycolysis is enhanced in kidney during IRI. (**a**) Concentrations of urinary metabolites involved in glycolysis. In the schematic diagram of glycolysis, a single arrow represents a one-step reaction, double arrows represent multi-step reactions. Red circles indicate upregulated metabolites. (**b**) HK2 mRNA expression in the kidneys at 24 h after ischemia reperfusion. (**c**) Western blot analysis of HK2 and PFKP expression in the kidneys at 6, 12 and 24 h after ischemia reperfusion. (**d**) Immunofluorescence staining of HK2 in mouse kidneys. Scale bar 100 μm. $^{*}P < .05$, $^{**}P < .01$, $^{***}P < .001$.

higher than combined five traditional clinical indicators (age, gender, diabetes mellitus, low ejection fraction and eGFR) [34].

In the present study, by urine metabolomics, we presented different urine metabolomic profiles between the AKI group and non-AKI group, and identified several differential metabolites, such as L-tryptophan, D-glucose-1-phosphate, propionyl-carnitine, indole, cellobiose, betaine and so on, which exhibited robust associations with clinical biochemical markers including Scr, BUN and eGFR. Meanwhile, potential biomarkers for CS-AKI were identified, such as L-tryptophan and indole, which had higher capacity in prediction of AKI than NGAL in patients undergoing cardiac surgery. Tryptophan is one of the essential amino acids. Tryptophan metabolism pathway mainly includes kynurenine, 5-hydroxytryptophan and indole pathways. Studies found that abnormal tryptophan metabolism contributed to the occurrence and progression of AKI [35]. Nicotinamide adenine dinucleotide (NAD+) could be *de novo* synthesized from L-tryptophan through the kynurenine pathway, which was impaired in the early stage of AKI [36]. Zhai *et al.*'s research also discovered this phenomenon in 3D cultured renal TECs [37]. Bajaj *et al.* found that urinary tryptophan and its kynurenine metabolites were significantly higher in cirrhotic patients complicated with AKI than in those without AKI [38].

Alterations in metabolites associated with energy metabolism, for example, anaerobic glycolysis–related metabolites D-glucose-1-phosphate and beta-D-fructose-6-phosphate were upregulated, and fatty acid metabolism– and TCA cycle–related metabolites L-carnitine, caprylic acid, fumaric acid and *cis*-aconitic acid were significantly downregulated, suggested renal metabolic reprogramming in the context of AKI, encompassing the activation of anaerobic glycolysis, compromised TCA cycle, and perturbed FAO. Research showed that carnitine insufficiency was correlated to AKI in a clinical study through inhibiting FAO. Administering L-carnitine to mice improved mitochondrial respiratory function and renal outcomes [39]. Li *et al.*'s study found that metabolic reprogramming could cause cell damage, inflammation and fibrosis, which might contribute to AKI occurrence and progression [40].

Under physiological conditions, proximal tubular epithelial cells primarily rely on FAO for energy production [41]. Glutamine and pyruvate can also serve as substrates for ATP generation through aerobic respiration [42]. However, limited hexokinase activity minimizes glucose utilization via glycolysis. Notably, the S3 segment of proximal TECs demonstrates heightened vulnerability to energy deficits under hypoxic conditions, owing to its restricted anaerobic glycolytic capacity and reduced oxygen partial pressure in the outer medulla [43]. Our metabolomic analysis revealed elevated levels of specific glycolytic metabolites, such as D-glucose-1-phosphate and fructose-6-phosphate, in the urine of AKI patients. In mice, both HK2 and PFKP, two pivotal rate-limiting enzymes in glycolysis, exhibited heightened expression in kidney during IRI, indicating enhanced glycolytic activity.

L-Carnitine primarily functions by esterifying carboxylic acids, thus facilitating fatty acid transport. In this study, AKI patients exhibited reduced level of urinary L-carnitine,

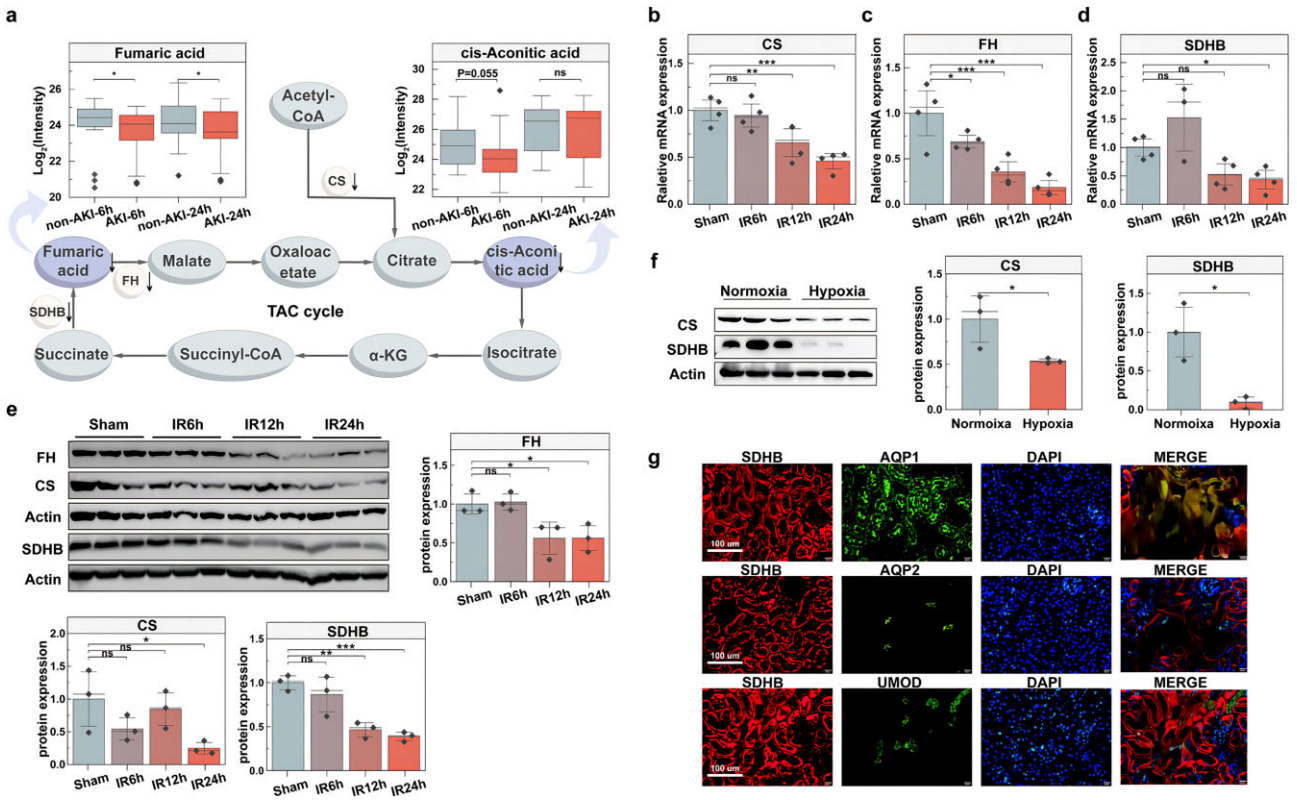

Figure 7: TCA cycle is impaired in kidney during IRI. (a) Concentrations of urinary metabolites involved in TCA cycle. Schematic diagram shows the TCA cycle pathway. Purple circles indicate metabolites that were reduced in the AKI-6h group. (b–d) qPCR analysis of citrate synthase (b), FH (c) and SDHB (d) in mouse kidneys after ischemia reperfusion. (e) Western blot analysis of kidney citrate synthase, FH and SDHB expression after ischemia reperfusion. (f) Western blot and qPCR analysis of citrate synthase and SDHB after hypoxia and reoxygenation. (g) Immunofluorescence staining of SDHB. $^{*}P < .05$, $^{**}P < .01$, $^{***}P < .001$. CS indicates citrate synthase here.

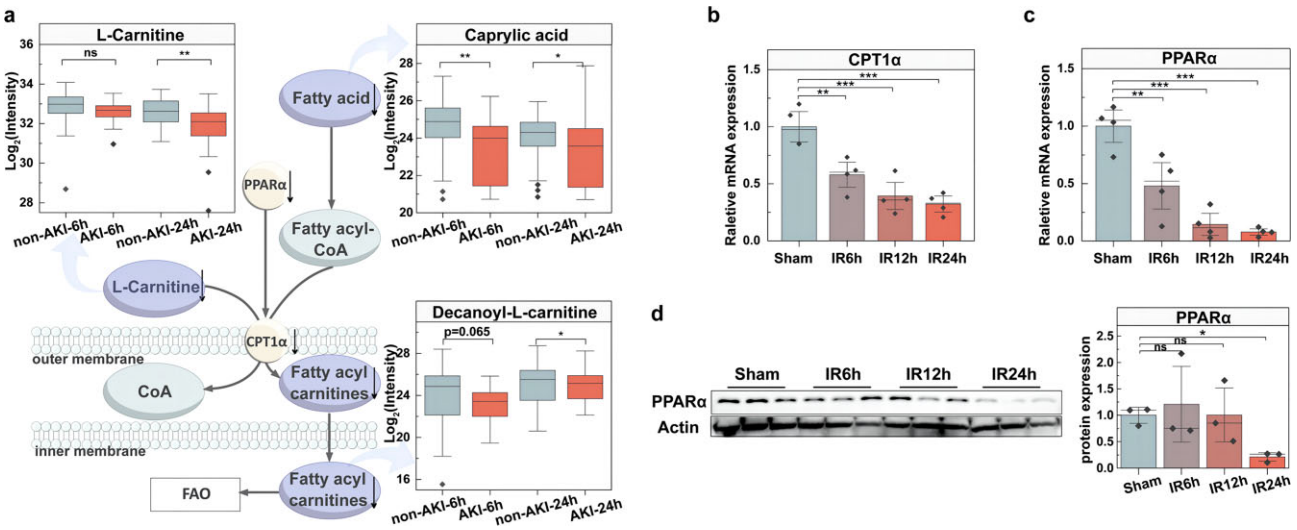

Figure 8: Fatty acid β-oxidation is impaired in kidney during IRI. (a) Concentrations of urinary metabolites involved in FAO. Schematic diagram shows the procedure of fatty acids β-oxidation. (b, c) qPCR analysis indicated a significant downregulation of CPT1α and PPARα mRNA in the kidneys of AKI mice. (d) Western blot analysis of kidney PPARα expression after ischemia reperfusion. $^{*}P < .05$, $^{**}P < .01$, $^{***}P < .001$.

particularly pronounced at 24 h post–cardiac surgery. The transfer of fatty acids into mitochondria involves L-carnitine acetyltransferases, catalyzing reversible acyl group interchanges between acetyl-coenzyme A (CoA) and L-carnitine, converting acyl-CoA esters to acyl-carnitine esters [44]. In our AKI mouse model, we demonstrated decreased CPT1α expression in kidney, a pivotal acylcarnitine transferase essential for medium- and long-chain fatty acid transportation to mitochondria. The

reduction of L-carnitine and CPT1α hinders fatty acid transport, subsequently impacting the efficiency of fatty acid oxidation. Consistently, our metabolomic analysis identified a significant decrease in acyl-carnitines associated with fatty acid metabolism in the urine of AKI patients. Specifically, a reduction in decanoyl carnitine, a medium-chain acylcarnitine, was observed in AKI. This decline could be attributed to limited carnitine availability, hindering fatty acid transport. In addition, the TCA cycle, situating downstream of aerobic glycolysis and fatty acid β-oxidation, showed impaired activity in kidney during AKI, characterized by the downregulation of citrate synthase, the pivotal enzyme regulating the TCA cycle, and SDHB, responsible for catalyzing the transformation of succinic acid to fumaric acid. Consistently, the levels of fumaric and *cis*-aconitic acids were significantly decreased in urine of AKI patients.

Limitations

There are several limitations to this study. First, the number of patients participated in this study is limited, and there was a lack of correlation analysis between urine metabolites and long-term prognosis of CS-AKI patients in this study. Secondly, though non-targeted metabolomics could detect more metabolites at the same time, using targeted metabolomics might be more accurate which should be considered in the future. Insufficient mechanism explanation may limit the generalizability of this model. Future study with diverse populations is warranted to further inspect urine metabolomics in AKI and validate this predictive model.

CONCLUSIONS

In this study, urine metabolomics was used to explore the changes of urine metabolites in the early stage of CS-AKI. Results implied the phenomenon of metabolic reprogramming during AKI, which was further confirmed in animal experiments. We also found that single urine metabolite had good predictive value in CS-AKI, while two metabolites combined had better predictive value. In summary, urine metabolites are potential noninvasive biomarkers of CS-AKI.

SUPPLEMENTARY DATA

Supplementary data are available at *Clinical Kidney Journal* online.

FUNDING

This work was supported by grants from Clinical Research Plan of Shanghai ShenKang Hospital Development Center (No. SHDC2020CR2022B), the National Natural ScienceFoundation of China grants 82170695 (to P.J.), the Special Fund for Clinical Research of Zhongshan Hospital, Fudan University, 2018; Science and Technology Commission of Shanghai (14DZ2260200), Shanghai Municipal Key Clinical Specialty (shslczdzk02501), Shanghai Municipal Hospital Frontier Technology Project supported by Shanghai ShenKang Hospital Development Center (SHDC12018127), Shanghai 'science and technology innovation plan' technical standard project (19DZ2205600), Shanghai 'science and technology innovation plan' Yangtze River Delta scientific and technological Innovation Community project (21002411500).

AUTHORS' CONTRIBUTIONS

P.J. and X.D. conceived and designed research; P.J., Q.Z., J.F., X.Z., T.R., Z.Z., C.T. and Q.S. performed experiments; P.J., Q.Z. and J.F. analyzed data, interpreted results of experiments, prepared figures and drafted the manuscript; X.D. and P.J. edited and revised manuscript.

DATA AVAILABILITY STATEMENT

All data generated or analyzed during this study are included in this article and its Supplementary data files. Further enquiries can be directed to the corresponding author.

CONFLICT OF INTEREST STATEMENT

None declared.

REFERENCES

1. Hu J, Chen R, Liu S *et al.* Global incidence and outcomes of adult patients with acute kidney injury after cardiac surgery: a systematic review and meta-analysis. *J Cardiothorac Vasc Anesth* 2016;**30**:82–9. https://doi.org/10.1053/j.jvca.2015.06.017
2. Boyer N, Eldridge J, Prowle JR *et al.* Postoperative acute kidney injury. *Clin J Am Soc Nephrol* 2022;**17**:1535–45. https://doi.org/10.2215/CJN.16541221
3. Blinder JJ, Goldstein SL, Lee VV *et al.* Congenital heart surgery in infants: effects of acute kidney injury on outcomes. *J Thorac Cardiovasc Surg* 2012;**143**:368–74. https://doi.org/10.1016/j.jtcvs.2011.06.021
4. Kork F, Balzer F, Spies CD *et al.* Minor postoperative increases of creatinine are associated with higher mortality and longer hospital length of stay in surgical patients. *Anesthesiology* 2015;**123**:1301–11. https://doi.org/10.1097/ALN.0000000000000891
5. Liu KD, Goldstein SL, Vijayan A *et al.* AKI!Now initiative: recommendations for awareness, recognition, and management of AKI. *Clin J Am Soc Nephrol* 2020;**15**:1838–47. https://doi.org/10.2215/CJN.15611219
6. Zhang J, Han J, Liu J *et al.* Clinical significance of novel biomarker NGAL in early diagnosis of acute renal injury. *Exp Ther Med* 2017;**14**:5017–21. https://doi.org/10.3892/etm.2017.5150
7. Wen Y, Parikh CR. Current concepts and advances in biomarkers of acute kidney injury. *Crit Rev Clin Lab Sci* 2021;**58**:354–68. https://doi.org/10.1080/10408363.2021.1879000
8. Vanmassenhove J, Vanholder R, Nagler E *et al.* Urinary and serum biomarkers for the diagnosis of acute kidney injury: an in-depth review of the literature. *Nephrol Dial Transplant* 2013;**28**:254–73. https://doi.org/10.1093/ndt/gfs380
9. Haase M, Bellomo R, Devarajan P *et al.* Accuracy of neutrophil gelatinase-associated lipocalin (NGAL) in diagnosis and prognosis in acute kidney injury: a systematic review and meta-analysis. *Am J Kidney Dis* 2009;**54**:1012–24. https://doi.org/10.1053/j.ajkd.2009.07.020
10. Vandenberghe W, De Loor J, Hoste EA. Diagnosis of cardiac surgery-associated acute kidney injury from functional to damage biomarkers. *Curr Opin Anaesthesiol* 2017;**30**:66–75. https://doi.org/10.1097/ACO.0000000000000419

11. Wang Y, Bellomo R. Cardiac surgery-associated acute kidney injury: risk factors, pathophysiology and treatment. *Nat Rev Nephrol* 2017;**13**:697–711. https://doi.org/10.1038/nrneph.2017.119
12. Grison S, Favé G, Maillot M *et al*. Metabolomics identifies a biological response to chronic low-dose natural uranium contamination in urine samples. *Metabolomics* 2013;**9**:1168–80. https://doi.org/10.1007/s11306-013-0544-7
13. Kim K, Aronov P, Zakharkin SO *et al*. Urine metabolomics analysis for kidney cancer detection and biomarker discovery. *Mol Cell Proteomics* 2009;**8**:558–70. https://doi.org/10.1074/mcp.M800165-MCP200
14. Khamis MM, Adamko DJ, El-Aneed A. Mass spectrometric based approaches in urine metabolomics and biomarker discovery. *Mass Spectrom Rev* 2017;**36**:115–34. https://doi.org/10.1002/mas.21455
15. Zelena E, Dunn WB, Broadhurst D *et al*. Development of a robust and repeatable UPLC-MS method for the long-term metabolomic study of human serum. *Anal Chem* 2009;**81**:1357–64. https://doi.org/10.1021/ac8019366
16. Want EJ, Masson P, Michopoulos F *et al*. Global metabolic profiling of animal and human tissues via UPLC-MS. *Nat Protoc* 2013;**8**:17–32. https://doi.org/10.1038/nprot.2012.135
17. Smith CA, Want EJ, O'Maille G *et al*. XCMS: processing mass spectrometry data for metabolite profiling using nonlinear peak alignment, matching, and identification. *Anal Chem* 2006;**78**:779–87. https://doi.org/10.1021/ac051437y
18. Navarro-Reig M, Jaumot J, García-Reiriz A *et al*. Evaluation of changes induced in rice metabolome by Cd and Cu exposure using LC-MS with XCMS and MCR-ALS data analysis strategies. *Anal Bioanal Chem* 2015;**407**:8835–47. https://doi.org/10.1007/s00216-015-9042-2
19. Horai H, Arita M, Kanaya S *et al*. MassBank: a public repository for sharing mass spectral data for life sciences. *J Mass Spectrom* 2010;**45**:703–14. https://doi.org/10.1002/jms.1777
20. Sud M, Fahy E, Cotter D *et al*. LMSD: LIPID MAPS structure database. *Nucleic Acids Res* 2007;**35**:D527–32. https://doi.org/10.1093/nar/gkl838
21. Abdelrazig S, Safo L, Rance GA *et al*. Metabolic characterisation of *Magnetospirillum gryphiswaldense* MSR-1 using LC-MS-based metabolite profiling. *RSC Adv* 2020;**10**:32548–60. https://doi.org/10.1039/D0RA05326K
22. Ogata H, Goto S, Sato K *et al*. KEGG: Kyoto Encyclopedia of Genes and Genomes. *Nucleic Acids Res* 1999;**27**:29–34. https://doi.org/10.1093/nar/27.1.29
23. Gagnebin Y, Tonoli D, Lescuyer P *et al*. Metabolomic analysis of urine samples by UHPLC-QTOF-MS: impact of normalization strategies. *Anal Chim Acta* 2017;**955**:27–35. https://doi.org/10.1016/j.aca.2016.12.029
24. Jia P, Wu X, Pan T *et al*. Uncoupling protein 1 inhibits mitochondrial reactive oxygen species generation and alleviates acute kidney injury. *EBioMedicine* 2019;**49**:331–40. https://doi.org/10.1016/j.ebiom.2019.10.023
25. Xu S, Jia P, Fang Y *et al*. Nuclear farnesoid X receptor attenuates acute kidney injury through fatty acid oxidation. *Kidney Int* 2022;**101**:987–1002. https://doi.org/10.1016/j.kint.2022.01.029
26. Jia P, Xu S, Ren T *et al*. LncRNA IRAR regulates chemokines production in tubular epithelial cells thus promoting kidney ischemia-reperfusion injury. *Cell Death Dis* 2022;**13**:562. https://doi.org/10.1038/s41419-022-05018-x
27. Badawy AA. Kynurenine pathway of tryptophan metabolism: regulatory and functional aspects. *Int J Tryptophan Res* 2017;**10**:1178646917691938. https://doi.org/10.1177/1178646917691938
28. Adeva-Andany MM, González-Lucán M, Donapetry-García C *et al*. Glycogen metabolism in humans. *BBA Clin* 2016;**5**:85–100. https://doi.org/10.1016/j.bbacli.2016.02.001
29. Pilkis SJ, Claus TH, Kurland IJ *et al*. 6-Phosphofructo-2-kinase/fructose-2,6-bisphosphatase: a metabolic signaling enzyme. *Annu Rev Biochem* 1995;**64**:799–835. https://doi.org/10.1146/annurev.bi.64.070195.004055
30. Wishart DS. Emerging applications of metabolomics in drug discovery and precision medicine. *Nat Rev Drug Discov* 2016;**15**:473–84. https://doi.org/10.1038/nrd.2016.32
31. Bai Y, Zhang H, Wu Z *et al*. Use of ultra high performance liquid chromatography with high resolution mass spectrometry to analyze urinary metabolome alterations following acute kidney injury in post-cardiac surgery patients. *J Mass Spectrom Adv Clin Lab* 2022;**24**:31–40. https://doi.org/10.1016/j.jmsacl.2022.02.003
32. Barrios C, Spector TD, Menni C. Blood, urine and faecal metabolite profiles in the study of adult renal disease. *Arch Biochem Biophys* 2016;**589**:81–92. https://doi.org/10.1016/j.abb.2015.10.006
33. Izquierdo-Garcia JL, Nin N, Cardinal-Fernandez P *et al*. Identification of novel metabolomic biomarkers in an experimental model of septic acute kidney injury. *Am J Physiol Renal Physiol* 2019;**316**:F54–62. https://doi.org/10.1152/ajprenal.00315.2018
34. Tian M, Liu X, Chen L *et al*. Urine metabolites for preoperative prediction of acute kidney injury after coronary artery bypass graft surgery. *J Thorac Cardiovasc Surg* 2023;**165**:1165–75.e3. https://doi.org/10.1016/j.jtcvs.2021.03.118
35. Kalim S, Rhee EP. An overview of renal metabolomics. *Kidney Int* 2017;**91**:61–9. https://doi.org/10.1016/j.kint.2016.08.021
36. Poyan Mehr A, Tran MT, Ralto KM *et al*. De novo NAD(+) biosynthetic impairment in acute kidney injury in humans. *Nat Med* 2018;**24**:1351–9. https://doi.org/10.1038/s41591-018-0138-z
37. Zhai Y, Chavez JA, D'Aquino KE *et al*. Kynurenine 3-monooxygenase limits de novo NAD(+) synthesis through dietary tryptophan in renal proximal tubule epithelial cell models. *Am J Physiol Cell Physiol* 2024;**326**:C1423–36. https://doi.org/10.1152/ajpcell.00445.2023
38. Bajaj JS, Garcia-Tsao G, Reddy KR *et al*. Admission urinary and serum metabolites predict renal outcomes in hospitalized patients with cirrhosis. *Hepatology* 2021;**74**:2699–713. https://doi.org/10.1002/hep.31907
39. Goto H, Nakashima H, Mori K *et al*. l-Carnitine pretreatment ameliorates heat stress-induced acute kidney injury by restoring mitochondrial function of tubular cells. *Am J Physiol Renal Physiol* 2024;**326**:F338–51. https://doi.org/10.1152/ajprenal.00196.2023
40. Li Z, Lu S, Li X. The role of metabolic reprogramming in tubular epithelial cells during the progression of acute kidney injury. *Cell Mol Life Sci* 2021;**78**:5731–41. https://doi.org/10.1007/s00018-021-03892-w
41. van der Rijt S, Leemans JC, Florquin S *et al*. Immunometabolic rewiring of tubular epithelial cells in kidney disease. *Nat Rev Nephrol* 2022;**18**:588–603. https://doi.org/10.1038/s41581-022-00592-x
42. Bhargava P, Schnellmann RG. Mitochondrial energetics in the kidney. *Nat Rev Nephrol* 2017;**13**:629–46. https://doi.org/10.1038/nrneph.2017.107

43. Scholz H, Boivin FJ, Schmidt-Ott KM *et al*. Kidney physiology and susceptibility to acute kidney injury: implications for renoprotection. *Nat Rev Nephrol* 2021;**17**:335–49. https://doi.org/10.1038/s41581-021-00394-7

44. Dambrova M, Makrecka-Kuka M, Kuka J *et al*. Acylcarnitines: nomenclature, biomarkers, therapeutic potential, drug targets, and clinical trials. *Pharmacol Rev* 2022;**74**:506–51. https://doi.org/10.1124/pharmrev.121.000408

Received: 25.1.2024; Editorial decision: 1.7.2024